RESEARCH PAPER

Artificial neural network approach for the prediction of terminal falling velocity of non-spherical particles through Newtonian and non-Newtonian fluids

A. Mirvakili[1], H. Roohian[2], S.Chahibakhsh[1]

[1]*Chemical Engineering Department, Faculty of Petroleum, Gas and Petrochemical Engineering, Persian Gulf University, Bushehr, Iran 75169-13817*

[2]*Environmental Research Center for petroleum and Petrochemical industries, School of Chemical and Petroleum Engineering, Shiraz University, Shiraz 71345, Iran*

ARTICLE INFO

Article History:
Received 10 April 2019
Revised 18 July 2019
Accepted 25 July 2019

Keywords:
Artificial Neural Networks
Terminal falling velocity
Non-spherical particles
non-Newtonian fluids

ABSTRACT

The investigation of the terminal falling velocity of non-spherical particles is currently one of the most promising topics in sedimentation technology due to its great significance in many separation processes. In this study, the potential of Artificial Neural Networks (ANNs) for the prediction of non-spherical particles terminal falling velocity through Newtonian and non-Newtonian (power law) liquids was investigated using 361 experimental data. ANNs emerged as the most popular non-linear mathematical models due to their good prediction, simplicity, flexibility and the large capacity which moderate engineering endeavor, and the availability of a large number of training algorithms. The developed ANN model demonstrated the acceptable values for the prediction of terminal falling velocities such as the determination coefficient (R2), MSE, and MRE which were equal to 0.9729, 0.0023, and 21%, respectively. In an investigation on terminal falling velocity and drag coefficient of spherical and non-spherical particles, it was found that the terminal falling velocity of non-spherical particles to spherical particles was 0.1.

How to cite this article
Mirvakili A, Roohian H, Chahibakhsh S. Artificial neural network approach for the prediction of terminal falling velocity of non-spherical particles through Newtonian and non-Newtonian fluids. Journal of Oil, Gas and Petrochemical Technology, 2019; 5(2): 1-14. DOI: 10.22034/JOGPT

1. INTRODUCTION

The settling rate of suspension plays an important role in many natural and industrial multiphase flows such as particles transport, liquid-solid separations and classification equipment, fixed bed reactors, and fluidized bed reactors. The movement type of a single solid particle in Newtonian and non-Newtonian liquids is well-known; after a short acceleration time, it will fall at its terminal settling velocity [1]. Indeed, the free settling velocity of particles plays a central role in processes involving relative motion between solid particles and a viscous medium. It is readily recognized that the free settling velocity is strongly influenced by the shape and orientation of particles, as well as the usual physical dimensions and properties of a given liquid/solid particles combination [2]. While it is readily acknowledged that the most practical applications entail hindered settling conditions, experience has shown that the knowledge of the single particle falling velocity often serves as a useful starting point. Therefore, over the years, considerable works have been reported on formulating reliable and accurate predictive schemes for the estimation of the drag force on a

* *Corresponding Author Email: mirvakili@pgu.ac.ir*
mirvakili96@gmail.com

particle and/or the free falling velocity of particles in fluids [3]. Although very few applications entail the use of perfectly spherical particles, a significant portion of available literature on this topic focuses on spherical particles in both Newtonian and non-Newtonian liquids [4-7]. The prediction of the terminal velocity of solid spheres falling through stagnant pseudo plastic fluids is required in several applications such as oil well drilling, geothermal drilling, transportation of non-Newtonian slurries and mineral processing.

1.1. Literature review

Cheng [8] proposed two formulas for the explicit evaluation of drag coefficient and settling velocity of spherical particles in the entire subcritical region. In comparison with fourteen previously-developed formulas, their study gave the best representation of a complete historical data set reported in the literature for Reynolds numbers up to 2×10^5. Arsenijević et al. [9] conducted an experimental investigation on the steady settling of spheres in quiescent media in a range of cylindrical tubes to ascertain the wall effects over a relatively wide range of Reynolds number values. For practical considerations, the retardation effect is important when the ratio of the particle diameter to the tube diameter (λ) is higher than about 0.05 and the drag coefficient for rising particles in co-current water flow increases with increasing water velocity. In a study of Rotondi [10], the settling velocity of a single sphere in a viscous suspension, neutrally buoyant spheres, for dilute and semi-dilute conditions was investigated. Their results in dilute conditions were in broad agreement with Batchelor's theoretical predictions.

Madhav and Chhabra [11] reported their experimental results (675 individual data points) of the free fall velocity of numerous cylinders, needles and rectangular prisms falling with their major axis parallel to the direction of gravity in shear thinning polymer solutions. In another related work, Madhav and Chhabra [2] measured the terminal settling velocity of non-spherical particles (i.e.cylinders, needles, and rectangular prisms) in 3 Newtonian liquids. Terminal velocity data (corrected for wall effects) were correlated using 2 approaches, the usual drag coefficient-Reynolds number relationship and a dimensionless velocity factor denoting the departure from the behavior of an equivalent sphere.

In another study, Chhabra [12] examined the effect of confining boundaries on the free falling velocity of variously shaped rigid particles in quiescent non-Newtonian shear thinning polymer solutions by Non-spherical particles made of different materials (1200-8000 kg/m^3) in different sizes which were sedimented in polymer solutions in cylindrical tubes with diameter range of 20-100 mm. The hindrance effect of the wall in terms of a wall factor as a function of particle size, shape and tube diameter in the streamline region ($Re < \sim 6\text{-}7$) was also quantified.

Xie and Zhang [13] examined the relationship between the Stokes shape factor and drag coefficient of non-spherical particles and particle sphericity, based on the experimental results in the laminar regime.

Wang et al. [14] presented data for the motion of cuboids with a square base in static glycerin–water solutions of various volume concentrations. They obtained a dimensionless expression for the terminal velocity as a function of Archimedes number (Ar), which is used to develop an accurate correlation for friction factor (CD) with an accuracy of 7.9% compared to experimental data, in the literature. Recently, Bagheri and Bonadonna [15] presented a new general model for the prediction of the drag coefficient of non-spherical solid particles of regular and irregular shapes falling in gas or liquid for sub-critical particle Reynolds numbers (i.e. $Re < 3 \times 10^5$). The new correlation was based on the particle Reynolds number and the two new shape descriptors were defined as a function of particle flatness, elongation, and diameter. New shape descriptors were easy-to-measure and could be more easily characterized than the sphericity. Xu et al. [16] investigated shape effects on the drag coefficient of non-sphere particles. They selected several typical shapes of particles and used 3-D printers to build particle models. They used high speed cameras to record the whole process of particle settling. They found that experiment data of non-sphere particles show good agreement with the formulas. They presented that among the considered formulas, the proposed formula by Tran-Cong is the most accurate one. Tang et al. [17] focused on the study of the hydrodynamic properties of a spherical particle in ionic liquids, and a series of experiments were implemented in a cylindrical bubble column with three different diameters of spherical particles made of the borosilicate glass. They developed two novel empirical models of the drag coefficient (CD) between a spherical particle and ionic liquids in the range of particle's Reynolds numbers (Re) from 0.1 to 85.

Jin et al. [18] investigated the drag coefficient of

two biomass spherical particles in supercritical water. They used a two-particle model to study the drag coefficient and flow characteristics of supercritical water flow past biomass particle clusters in the range of 10<Re<200. They found that the interactions between particles can transmit larger perpendicular distances to the flow field at low Re. The drag coefficient of particles is mainly affected by the wake zone generated behind the upstream particles and nozzle effect between particles.

ANN models, compared to mathematical models, are able to learn the relationship between dependent and independent variables through the data without the need of developing specific functions between them [19]. ANNs have gained increasing popularity in different fields of engineering in the past few decades, because of their capability of extracting complex and nonlinear relationships.

Among few works which have been done on the terminal velocity prediction, Ghamari et al. [19] related seed settling velocities to particular seed properties like size, seed type, and moisture content using ANN model. Rooki et al. [20] also predicted the terminal velocity of solid spheres falling through Newtonian and non-Newtonian power law liquids.

1.2. Objective

The present article focused on the application of Artificial Neural Network for the prediction of the terminal falling velocity of non-spherical particles through Newtonian and non-Newtonian power law liquids. The terminal falling velocity of non-spherical particles through Newtonian and non-Newtonian power law has been experimentally investigated; however, this phenomenon has not been modeled by ANN. In this study, single layer feed forward Neural Networks with back propagation learning were constructed for the calculation of terminal velocity for non-spherical particles. 361 experimental data sets from the literature were represented in Table 1 and then 75% and 25% of data were used for the training and testing of the network performance respectively. Also, the network training and estimation values were investigated using the mean square error, mean relative error and correlation coefficient, as a statistical evaluation.

2. Artificial neural network

Artificial Neural Network (ANN) as a branch of the artificial intelligent systems was developed in the second half of the 20th century in order to imitate the biological structure of the human brain [21].

The topology of the ANN architecture is illustrated in Figure 1. Processing units, called neurons are inspired by the biological neurons. Inputs (x_r) coming from other neurons are multiplied by their corresponding weights (w_{kr}), and then summed up (N). After that, an activation function (Φ) is applied to the summation to calculate the output of that neuron which is ready to be transferred to other neurons [25]. In this network, each element of the input vector xr is connected to all neurons through the weighted matrix w_{kr}. The i th neuron has a collector which gathers its weighted inputs and bias to form its own scalar output N (i). The various N(i)s are taken form an n-element net input vector n. Finally, the neuron layer outputs form a column vector derived from equation (1):

$$n_j = \phi\ (\sum_{r=1}^{N} w_k\ \ x_r\ +\ b_j) \qquad (1)$$

Different types of transfer functions have been applied for ANNs, such as linear, log-sigmoid, tan-sigmoid, and radial basis transfer functions [26].

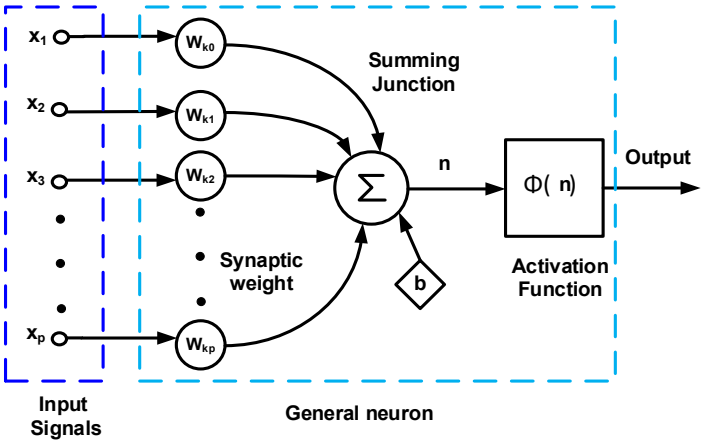

Figure 1. A typical neuron

2.1. Back Propagation Artificial Neural Network

Back Propagation Artificial Neural Network (BPANN) is commonly used in many fields, particularly in engineering because of its high learning capacity and simple algorithm. This algorithm aims to reduce errors backward. The BPANN uses the gradient steepest descent method to minimize energy functions. Because the multilayer artificial neural network has a nonlinear characteristic, it can be used to solve nonlinear equations or other complicated calculations [27]. Figure 2 shows the BP neural network which was first proposed by Rumelhart et al. in order to learn weight and yield values [28]. This method has been modified and utilized in the literature extensively [29-34].

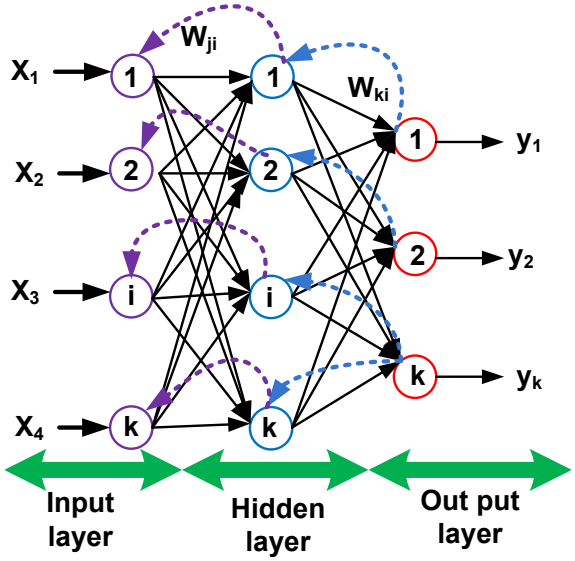

Figure 2. Neural network structure

2.2. Levenberg-Marquardt algorithm

In order to minimize the output errors, it is first essential to train the network and choose a weight update function between the layers based on the training data set. Various types of algorithms have been found to be effective for the adaptation of these weight values. Among these algorithms, the most popular ones are the Error Back Propagation method (EBP) and the Levenberg-Marquardt (LM) algorithm [35, 36].

Another neural network training algorithm is the LM algorithm. LM method is, in fact, an approximation of the Newton's method using the second-order derivatives of the cost function so that a better convergence behavior can be obtained [37]. This algorithm modifies the values of weights in a grouped manner, after the application of all the training vectors. It is one of the most effective training algorithms for the feed forward neural networks [35].

The changes in the values of the weights can be obtained using Equation (2):

$$\Delta w_{ij,n} = F_n + \alpha \ \Delta w_{j,n-1} \qquad (2)$$

In the LM algorithm, the update function, F_n, can be calculated using Equation (3):

$$F_n = -\left[J^T \times J + \mu I\right]^{-1} \times J^T \times e \qquad (3)$$

Where J is the Jacobian matrix that contains first derivatives of the network errors with respect to the weights, and e is a vector of the network errors [38].

2.3. Data collection and pre-processing

The feed-forward neural networks with LM algorithm is a very powerful optimization modeling. In this study, one-layer feed forward neural networks with LM algorithm were constructed for the calculation of terminal velocity for non-spherical particles. In the present work, 361 experimental data sets from the literature, represented in Table 1 in the appendix, were used.

The network inputs were the properties of the surrounding liquid such as density (ρ_f) and rheological parameters (k, n) as well as the properties of the spherical particles such as

density (ρ_p) and sphericity (ϕ_p). The network output was terminal velocity. In view of the neural computation algorithm requirements, the data of both inputs and outputs were normalized to an interval by a transformation process. In this research, normalization of data (inputs and outputs) was done for a range from −1 to 1 using Equation (4) [20]:

$$P_n = 2\frac{P - P_{\min}}{P_{\max} - P_{\min}} - 1 \quad (4)$$

Where P_n is the normalized parameter, P denotes the actual parameter, P_{min} and P_{max} represent the minimum and maximum of this parameter, respectively. In this study, 75% and 25% of data were used for training and testing of the network performance respectively. About 295 out of 361 data were selected as the train data and then 66 data were considered for the test, randomly. The statistical evaluation indices included the mean square error (MSE), mean relative error (MRE) and correlation coefficient (R^2) verify the network training and estimation results. A lower error shows that the estimated value of the network is closer to the true value, while higher R^2 indicates that the output and input values of the network tend to be closer. Therefore, both R^2 and error can represent the training quality indices of different meanings, with expressions as follows:

$$MSE = \sqrt{\frac{\sum_{i=1}^{n}(\upsilon_i - \hat{\upsilon}_i)^2}{n-1}} \quad (5)$$

$$MRE = \frac{1}{n}\sum_{i=1}^{n}\left(\frac{\left|\upsilon_i - \hat{\upsilon}_i\right|}{\upsilon_i}\right) \quad (6)$$

$$R^2 = 1 - \frac{\sum_{i=1}^{n}(\upsilon_i - \hat{\upsilon}_i)^2}{\sum_{i=1}^{n}\upsilon_i^{\,2} - \frac{\sum_{i=1}^{n}\hat{\upsilon}^2{}_i}{n}} \quad (7)$$

Where υ_i is the measured value, $\upsilon\hat{}i$ denotes the predicted value, and n stands for the number of samples. The best fitting between the measured and the predicted values would have a mean square error of zero and a determination coefficient equal to one. The selected ANN model in this study had one layer with five inputs (ρ_f, K, n, ϕ_p, ρ_p) and one hidden layer with 14 neurons. The neural network with a wide range of neurons was tested. Since 14 selected neurons were applied in this work, the root mean square error and determination coefficient became close to zero and one, respectively.

3. esults and discussion

The particular purpose of this study was introducing an ANN with LM algorithm which can predict the settling velocity of non-spherical particles considering different inputs (such as ρ_f, K, n, ϕ_p, ρ_p). Factors affecting the performance of the desired ANN will be discussed in the present section.

The input matrix in the training step is a 5×295 matrix, where 5 is the number of network inputs, and 295 is the number of samples used to train the network. In this case study, five input variables (ρ_f, K, n, ϕ_p, ρ_p) were used and there was only one network outputs (terminal velocity), so the outputs matrix in the training step, was a 1×295 matrix, while the inputs matrix for testing phase and the output matrix were 5×66 and 1×66, respectively.

The important factors for evaluating the effectiveness of network are MSE (mean squared error) of the training data set, MRE (mean relative error) of testing data set and the coefficient of determination (R^2). These parameters are affected by the number of data sets (N) and the number of parameters in the model.

Figure 3 illustrates the agreement between the ANNs input and output. The obtained result is a typical linear relation with a determination coefficient close to 1. In Figure 3, the predicted velocities are compared with the measured data for 295 training data sets. Results showed the perfect fitting because the determination coefficient (R^2), MSE, and MRE are 0.9729, 0.0023, and 21%, respectively. Also, there was a good agreement between the MSE and MRE errors of input and output of the ANN which means that the trained neural networks can predict the values of terminal velocity of non-spherical particles in Newtonian and non-Newtonian fluid admissibly.

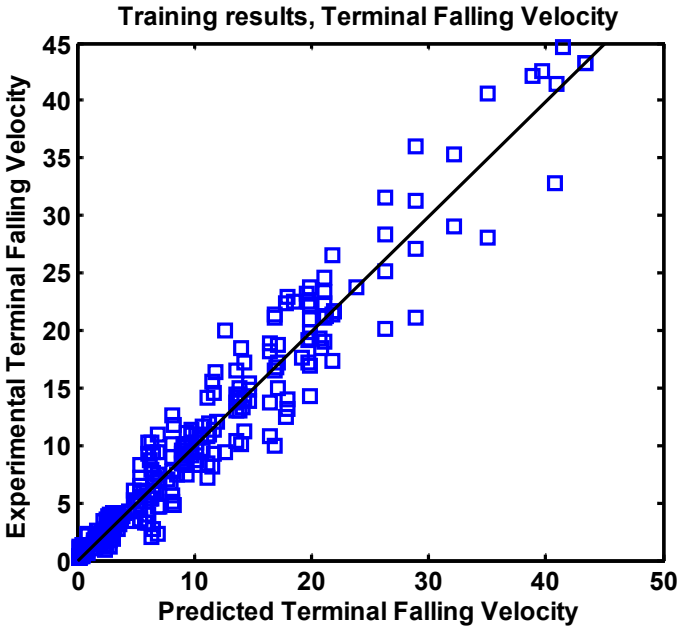

Figure 3. Comparison between the BPNN predictions and the measured terminal velocity for training data

The comparison of the network predictions with the measured values of the test data set is shown in Figure 4. The determination coefficient is 0.9253, the MSE is 0.011 and the MRE is 40% which indicate that although these predictions are not as well as the predictions done by the training data set from the engineering point of view, they still have an admissible accuracy. In the present study, the terminal velocity of different particles such as cubes, cylinders, needles, plates, and discs were used. Therefore, the difference in the terminal velocity of particles can arise from the difference in particle shapes. Although the dispersed distributions of terminal velocities lead to weak estimation, ANN which has the dispersed distributions of terminal velocities showed an acceptable accuracy in the prediction.

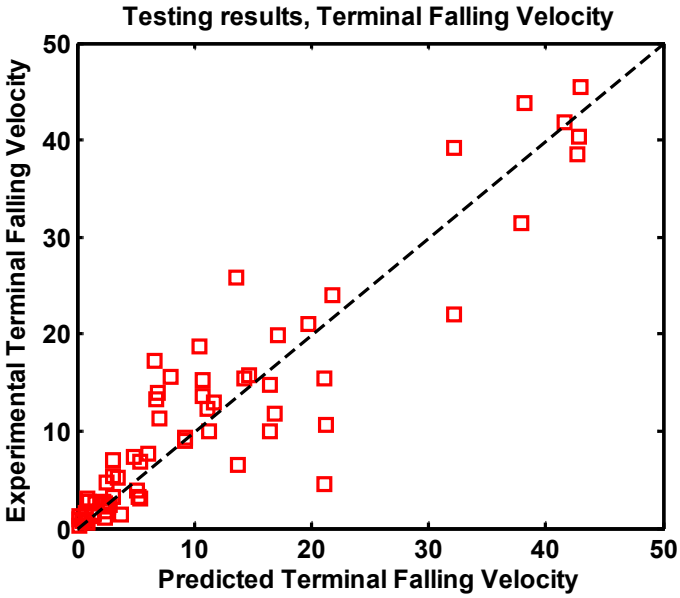

Figure4. Comparison between the BPNN predictions and the measured terminal velocity for test data

The results in Figure 5 were obtained by putting all the data (361 data) together and then comparing them with the measurements. This leads to a determination coefficient of 0.9599.

Moreover, Figure 6 shows an example of the convergence profile of neural network training. As it is shown, the network approximately reaches the considered goal (0.0023).

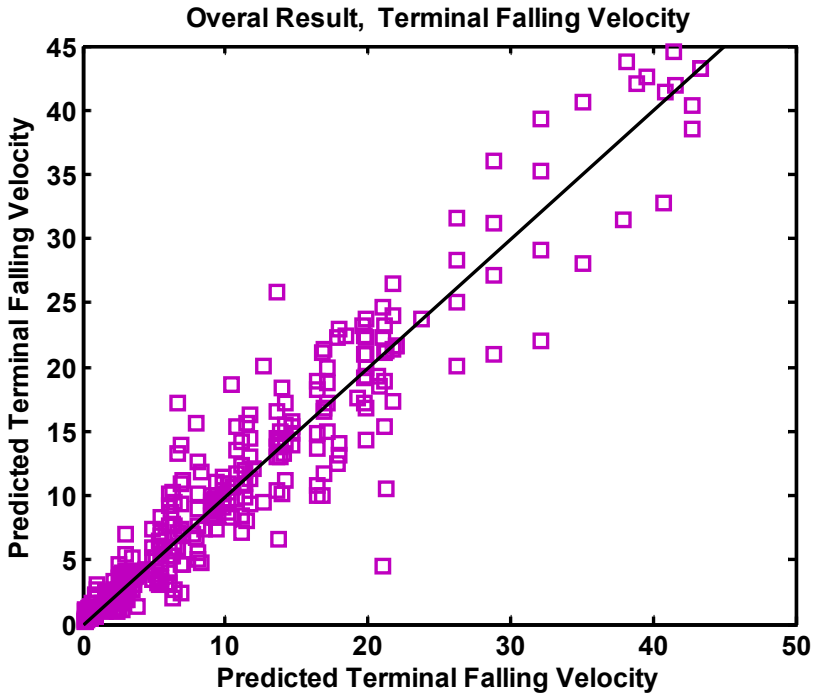

Figure 5. Comparison between the BPNN predictions and the measured terminal velocity for all data

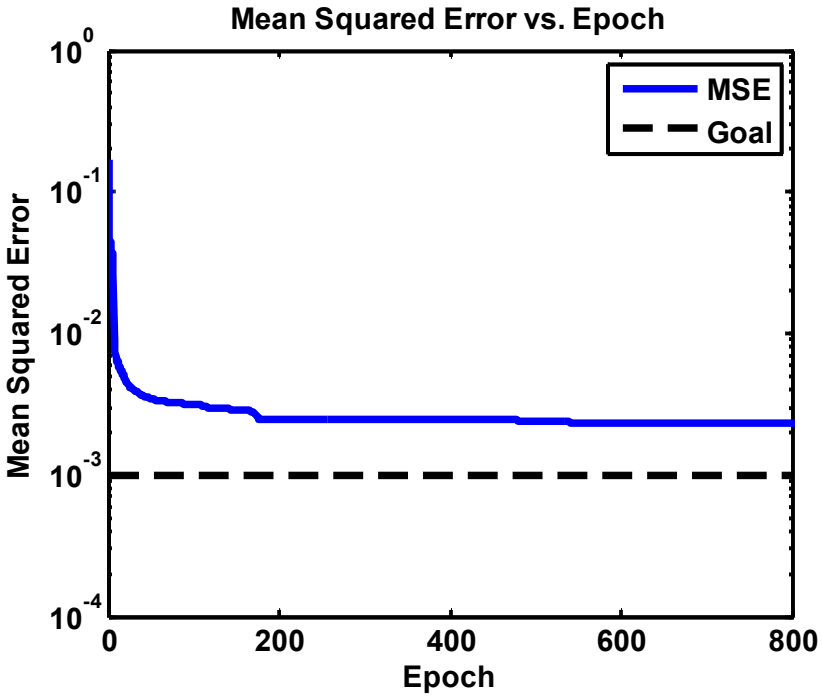

Figure 6. A convergence profile for neural network training

Figure 7 displays the network predictions and the measured velocity for test data using BPNN model. Moreover, the predicted data by ANN are compared with the experimental data in Table 2. Also, the average values of the error are presented. In addition, the proposed network shows an acceptable accuracy (1.39% average error) in predicting the terminal velocity of the non-spherical particles in the Newtonian and non-Newtonian fluids as illustrated in Table 2 and Figure 7.

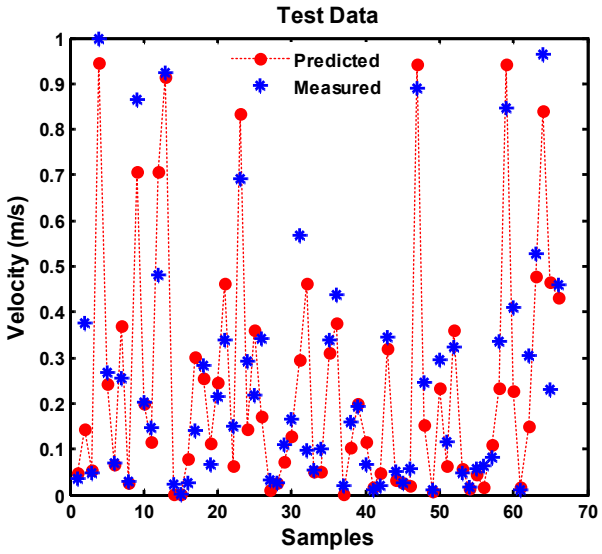

Figure 7. Comparison between the network predictions and the measured velocity for all data

Table 2. Comparative Artificial neural network output and measured velocity

Inputs					Output		
K (Pa.s^n)	n	P_f (Kg/m^3)	ϕ_p Sphercity	ρ_p (Kg/m^3)	Measured velocity (m/s)	Predicted velocity (m/s)	Errors(%)
0.003	0.003	0.9329	0.612252	0.003	0.702315	0.621263	-11.0464
0.26804	0.681827	0.405079	0.786436	0.186031	0.688335	0.712215	3.352921
0.469576	0.737621	0.405079	0.250451	0.916143	0.580593	0.584748	0.710549
0.26804	0.681827	0.405079	0.786436	0.114216	0.684774	0.701074	2.324936
0.556839	0.9329	0.324664	0.040261	0.88263	0.464097	0.474797	2.253546
0.266066	0.003	0.003	0.9329	0.030433	0.68524	0.69547	1.470956
0.527751	0.644631	0.405079	0.508412	0.186031	0.798154	0.746884	-6.86457
0.9329	0.9329	0.262524	0.288667	0.758631	0.468284	0.469336	0.224131
0.527751	0.644631	0.405079	0.479749	0.186031	0.752438	0.783388	3.950702
0.003	0.003	0.9329	0.665302	0.003	0.485666	0.595996	18.51198
0.257652	0.672528	0.405079	0.823697	0.186031	0.713671	0.71951	0.811544
0.226694	0.003	0.003	0.731118	0.026364	0.693651	0.714765	2.954028
0.26804	0.681827	0.405079	0.823697	0.186031	0.685521	0.716216	4.28568
0.9329	0.9329	0.262524	0.299177	0.758631	0.475545	0.469324	-1.32563
0.003	0.003	0.9329	0.634772	0.186414	0.862188	0.837604	-2.93495
0.083126	0.900354	0.405079	0.308731	0.758631	0.539953	0.558684	3.352789
0.556839	0.9329	0.324664	0.230387	0.134205	0.478095	0.513796	6.948424

0.083126	0.900354	0.405079	0.594398	0.006495	0.533478	0.529435	-0.76362
0.26804	0.681827	0.405079	0.747264	0.186031	0.686338	0.710811	3.442995
0.556839	0.9329	0.324664	0.517966	0.134205	0.566399	0.539603	-4.96582
0.083126	0.900354	0.405079	0.332616	0.758631	0.571429	0.56527	-1.0896
0.556839	0.9329	0.324664	0.476883	0.134205	0.47683	0.527624	9.626812
0.083126	0.900354	0.405079	0.623061	0.006495	0.491274	0.526794	6.742654
0.757335	0.727392	0.405079	0.60873	0.186031	0.656296	0.609319	-7.70969
0.083126	0.900354	0.405079	0.307776	0.758631	0.554934	0.558301	0.60313
0.257652	0.672528	0.405079	0.546628	0.186031	0.75466	0.752315	-0.31172
0.257652	0.672528	0.405079	0.642169	0.186031	0.707774	0.71745	1.348677
0.257652	0.672528	0.405079	0.697583	0.186031	0.703939	0.713953	1.402634
0.083126	0.900354	0.405079	0.642169	0.006495	0.517481	0.52523	1.475367
0.23968	0.003	0.003	0.201916	0.9329	0.697434	0.710674	1.862994
0.003	0.003	0.9329	0.682287	0.186414	0.875137	0.894479	2.162382
0.083126	0.900354	0.405079	0.41096	0.134205	0.666356	0.676299	1.470186
0.9329	0.9329	0.262524	0.582934	0.006495	0.478653	0.486444	1.601604
0.757335	0.727392	0.405079	0.298222	0.006495	0.611372	0.608003	-0.55421
0.527751	0.644631	0.405079	0.697583	0.186031	0.776823	0.696666	-11.5058
0.9329	0.9329	0.262524	0.848537	0.006495	0.504273	0.484658	-4.04719
0.083126	0.900354	0.405079	0.307776	0.758631	0.539953	0.558301	3.286484
0.228045	0.003	0.003	0.745353	0.032228	0.691031	0.715561	3.428033
0.23968	0.003	0.003	0.569558	0.802437	0.695188	0.719277	3.349005
0.469576	0.737621	0.405079	0.316374	0.880236	0.561767	0.616292	8.847229
0.469576	0.737621	0.405079	0.250451	0.916143	0.565652	0.584748	3.265727
0.757335	0.727392	0.405079	0.571469	0.186031	0.606691	0.618359	1.886982
0.26804	0.681827	0.405079	0.747264	0.114216	0.684899	0.701552	2.373738
0.083126	0.900354	0.405079	0.298222	0.758631	0.541875	0.553946	2.179133
0.23968	0.003	0.003	0.322871	0.802437	0.700682	0.712014	1.591523
0.083126	0.900354	0.405079	0.293444	0.758631	0.549943	0.551412	0.266404
0.003	0.003	0.9329	0.695537	0.186414	0.888086	0.901689	1.50859
0.556839	0.9329	0.324664	0.003	0.916143	0.463831	0.472369	1.807319
0.469576	0.737621	0.405079	0.312553	0.802437	0.610476	0.588075	-3.80924
0.26804	0.681827	0.405079	0.823697	0.186031	0.687752	0.716216	3.974148
0.9329	0.9329	0.262524	0.848537	0.006495	0.493346	0.484658	-1.79259
0.9329	0.9329	0.262524	0.299177	0.758631	0.480018	0.469324	-2.27858
0.257652	0.672528	0.405079	0.508412	0.186031	0.761433	0.76214	0.092769
0.9329	0.9329	0.262524	0.326884	0.758631	0.49484	0.469472	-5.40344
0.9329	0.9329	0.262524	0.336438	0.758631	0.47953	0.469581	-2.11871
0.003	0.003	0.9329	0.695529	0.003	0.698331	0.612286	-14.053
0.257652	0.672528	0.405079	0.747264	0.186031	0.727217	0.713811	-1.8781
0.083126	0.900354	0.405079	0.441533	0.134205	0.676815	0.753892	10.22379

0.003	0.003	0.9329	0.653491	0.186414	0.894063	0.8677	-3.0382
0.083126	0.900354	0.405079	0.506501	0.134205	0.768655	0.767301	-0.1765
0.757335	0.727392	0.405079	0.308731	0.006495	0.534474	0.627075	14.76715
0.9329	0.9329	0.262524	0.664143	0.006495	0.472109	0.48497	2.651928
0.003	0.003	0.9329	0.695535	0.043635	0.673927	0.680131	0.912191
0.26804	0.681827	0.405079	0.642169	0.114216	0.685392	0.697663	1.758873
0.220046	0.003	0.003	0.752805	0.031032	0.690273	0.715692	3.551718
0.757335	0.727392	0.405079	0.571469	0.186031	0.601013	0.618359	2.805172
0.257652	0.672528	0.405079	0.57529	0.114216	0.698924	0.694678	-0.61117
0.23968	0.003	0.003	0.34475	0.802437	0.69985	0.712203	1.734513
0.469576	0.737621	0.405079	0.468284	0.931703	0.557892	0.548843	-1.64877
0.083126	0.900354	0.405079	0.594398	0.006495	0.513855	0.529435	2.942779
0.9329	0.9329	0.262524	0.299177	0.758631	0.4719	0.469324	-0.54883
0.26804	0.681827	0.405079	0.594398	0.186031	0.694511	0.723646	4.026149
0.23968	0.003	0.003	0.394431	0.802437	0.703336	0.712982	1.352831
0.003	0.003	0.9329	0.691295	0.003	0.483673	0.608424	20.50388
0.083126	0.900354	0.405079	0.332616	0.758631	0.548021	0.56527	3.051455
0.757335	0.727392	0.405079	0.627838	0.006495	0.574836	0.617557	6.917741
0.757335	0.727392	0.405079	0.60873	0.186031	0.629152	0.609319	-3.25497
0.26804	0.681827	0.405079	0.670831	0.186031	0.690711	0.712165	3.012505
0.527751	0.644631	0.405079	0.670831	0.186031	0.783746	0.695357	-12.7113
0.757335	0.727392	0.405079	0.332616	0.006495	0.722088	0.688957	-4.80878
0.083126	0.900354	0.405079	0.332616	0.758631	0.559078	0.56527	1.095469
0.527751	0.644631	0.405079	0.697583	0.186031	0.540929	0.696666	22.35462
0.23968	0.003	0.003	0.182617	0.9329	0.699397	0.710623	1.57976
0.26804	0.681827	0.405079	0.747264	0.186031	0.689057	0.710811	3.060428
0.757335	0.727392	0.405079	0.298222	0.006495	0.646534	0.608003	-6.3374
0.083126	0.900354	0.405079	0.623061	0.006495	0.528946	0.526794	-0.40856
0.26804	0.681827	0.405079	0.546628	0.186031	0.696638	0.745462	6.549606
0.757335	0.727392	0.405079	0.332616	0.006495	0.696538	0.688957	-1.10031
0.257652	0.672528	0.405079	0.786436	0.186031	0.71898	0.715429	-0.49631
0.003	0.003	0.9329	0.634394	0.186414	0.737676	0.836876	11.85354

In Figure 8, the terminal velocities of non-spherical and spherical particles are compared. In this figure, the measured terminal velocities of non-spherical and spherical particles are shown versus the Reynolds number. The measured terminal velocities of spherical particles were presented by Rooki et al. [20] and the measured terminal velocities of non-spherical particles were selected from test data. As shown in Figure 8, the terminal velocities of spherical particles are higher than the non-spherical particles for all Reynolds numbers. It means that the spherical particles in Newtonian and non-Newtonian fluids will precipitate sooner than the non-spherical particles. As the shape differences impress the drag coefficient, it can be found that the reduction of non-spherical particles terminal falling velocity leads to the higher drag force on them in comparison with the spherical particles.

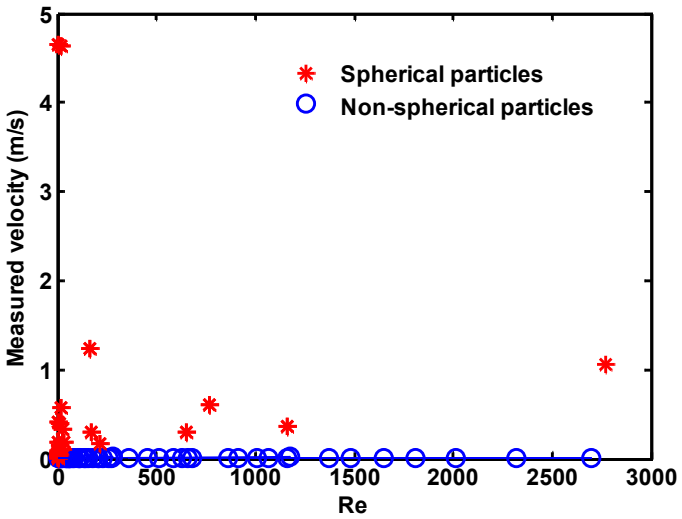

Figure 8. Comparison between the terminal velocities of spherical and the non-spherical particles

4. Conclusion

In this study, an artificial neural network (ANN) based on Back Propagation Algorithm was developed with a configuration including one hidden layer and 8 neurons. The ANN model was trained and tested using 361 experimental data of non-spherical particles terminal falling velocity. It was proved that the ANN approach can be considered as an alternative and practical technique to predict the terminal velocity of non-spherical particles, based on some independent variables such as particle density (ρ_p), particle sphericity (ϕ_p), fluid density (ρ_f) and rheological parameters (k, n). The ANN model can easily estimate the terminal velocity of non-spherical particles with input parameters in a proper range. The results obtained from the proposed ANN model data set were found to be satisfactory (determination coefficients were 97.29%, 92.53% and 95.99% for training data, test data, and all data, respectively) in comparison with those achieved by the tests. A comparison was also made between the terminal velocity and the drag coefficient of non-spherical particles and spherical particles and the results indicated that the terminal velocity of spherical particles is higher than the one of non-spherical particles, while their drag coefficient has a lower value compared with the non-spherical particles. Therefore, the drag force on non-spherical particles is higher than the one on spherical particles due to the main difference in their shape.

5. omenclature

Artificial Neural Networks	(ANNs)
friction factor	CD
Archimedes number	Ar
Back Propagation Artificial Neural Network	BPANN
Multi-Layer Perceptron	MLP
Generalized Regression Neural Network	GRNN
Radial Basis Neural Network	RBFNN
Levenberg-Marquardt	LM
Error Back Propagation method	EBP
mean square error	MSE
mean relative error	MRE
correlation coefficient	R2

6. References:

[1] Kelessidis VC «An explicit equation for the terminal velocity of solid spheres falling in pseudoplastic liquids», Chemical Engineering Science, 59, 4437 – 4447,2004.

[2] G. Venu Madhav, R.P. «Chhabra Drag on non-spherical particles in viscous fluids», International Journal of Mineral Processing, 43, 15-29,1995.

[3] P. Rajitha, R.P. Chhabra, N.E. Sabiri, J. «Comiti Drag on non-spherical particles in power law non-Newtonian media», International Journal of Mineral Processing, 78, 110– 121,2006.

[4] R.P. Chhabra "Bubbles, Drops and particles in non-Newtonian fluids", first ed., CRC Press, Florida. 1993.

[5] K. Ceylan, S. Herdem, T. Abbasov "A theoretical model for estimation of drag force in the flow of non-Newtonian fluids around spherical particles", Powder Technology, 102, 286– 292,1999.

[6] K.C. Wilson, R.R. Horsley, T. Kealy, J.A. Reizes, M. Horsley "Direct prediction of fall velocities in non-Newtonian materials", International Journal of Mineral Processing, 71, 17– 30, 2003.

[7] M. Renaud, E. Mauret, R.P. Chhabra "Power law fluid flow over a sphere: average shear rate and drag coefficient". Canadian Journal of Chemical Engineering, 82, 1066– 1070, 2004.

[8] N.S. Cheng "Comparison of formulas for drag coefficient and settling velocity of spherical particles", Powder Technology, 189, 395–398, 2009.

[9] Z.Lj Arsenijević, Ž.B. Grbavčić, R.V. Garić-Grulović, N.M. Bošković-Vragolović "Wall effects on the velocities of a single sphere settling in a stagnant and counter-current fluid and rising in a co-current fluid", Powder Technology, 203, 237–242, 2010.

[10] R.D. Felice, M. Rotondi "The settling velocity of a single sphere in viscous fluid: The effect of neighboring larger spheres", Powder Technology, 217, 486–488, 2012.

[11] G. Venu Madhav, R.P. Chhabra "Settling velocities of non-spherical particles in non-Newtonian polymer solutions", Powder Technology, 78, 77-83, 1994.

[12] R.P. Chhabra "Wall effects on terminal velocity of non-spherical particles in non-Newtonian polymer solutions", Powder Technology, 88, 39-44, 1996.

[13] H.Y. Xie, D.W. Zhang «Stokes shape factor and its application in the measurement of spherity of non-spherical particles», Powder Technology, 114, 102–105, 2001.

[14] J Wang, H Qi, J Zhu «Experimental study of settling and drag on cuboids with square base», Particuology 9, 298–305, 2011.

[15] B. Xu, N. Huang, W. He, Y. Chen "Investigation on terminal velocity and drag coefficient of particles with different shapes". Journal of Physics: Conf. Series 822 ,12047, 2017.

[16] Gh. Bagheri , C. Bonadonna "On the drag of freely falling non-spherical particles", Powder Technology, 301,526-544,2016.

[17] Q. Tang, X. Qin, H. Dong, X. Zhang, X. Wang, K. Wang " Novel drag coefficient models of ionic liquid - spherical particle system" Chemical Engineering Science, 31, 177-185, 2019.

[18] H.Jin, H. Wang, Z. Wu, Zh. Ren, Zh. Ou, "Numerical investigation on drag coefficient and flow characteristics of two biomass spherical particles in supercritical water" Renewable Energy,

138, 11-17, 2019.

[19] S. Ghamari, A.M. Borghei, H. Rabbani, J. Khazaei, F. Basati «Modeling the terminal velocity of agricultural seeds with artificial neural networks», African Journal of Agricultural Research, 5, 389-398, 2010

[20] R. Rooki, F. Doulati Ardejani, A. Moradzadeh, V.C. Kelessidis, M. Nourozi «Prediction of terminal velocity of solid spheres falling through Newtonian and non-Newtonian pseudoplastic power law fluid using artificial neural network», International Journal of Mineral Processing, 53–61, 2012.

[21] P. Viotti, G. Liuti, P.D. Genova «Atmospheric urban pollution: applications of an artificial neural network (ANN) to the City Peugia», Ecological Modelling,148, 27–46, 2002.

[22] C. Buratti, L. Barelli, E. Moretti «Application of artificial neural network to predict thermal transmittance of wooden windows», Applied Energy , 98, 425–432, 2012.

[23] S.A. Kalogirou «Applications of artificial neural-networks for energy systems.» Applied Energy, 67,17–35, 2000.

[24] R.M. Aghav, S. Kumar, S.N. Mukherjee «Artificial neural network modeling in competitive adsorption of phenol and resorcinol from water environment using some carbonaceous adsorbents.» Journal of Hazardous Material, 188, 67–77, 2011.

[25] H. Demuth, M. Beale «Neural Network Toolbox For Use with MATLAB», User's Guide Version 4, 2002.

[26] R. Raghavan, W. Chu, J.R. Jones «Practical considerations in the analysis of gas condensate well tests», SPE Paper 30576, 1995.

[27] M. Liu, Y. Yang, Q. Li, H. Zhang «Parallel computing of multi-scale continental deformation in the western united states: Preliminary results», Physics of Earth and Planeteray interiors ,163, 35–51, 2007.

[28] D.E. Rumelhart, G.E. Hinton, R.J. Williams «Learning representations by back-propagating errors», Nature, 323, 533–536, 1986.

[29] Z.H. Che «PSO-based back-propagation artificial neural network for product and mold cost estimation of plastic injection molding», Computers & Industrial Engineering, 58, 625–637, 2010.

[30] J.B. Wu, W.J. Li «Study on textile industry using BP neural networks». Program Text Science and Technology, 2, 7–10, 2007.

[31] M.P. Deosarkar, V.S. Sathe «Predicting effective viscosity of magnetite ore slurries by using artificial neural network», Powder Technology, 219, 264–270, 2012.

[32] Sh. Salar Behzadi, Ch. Prakasvudhisarn, J. Klocker, P. Wolschann, H. Viernstein «Comparison between two types of

Artificial Neural Networks used for validation of pharmaceutical processes», Powder Technology, 195, 150–157, 2009.

[33] Kh. Elsayed , Ch. Lacor «Modeling, analysis and optimization of aircyclones using artificial neural network, response surface methodology and CFD simulation approaches», Powder Technology, 212, 115–133, 2011.

[34] Y.D. Ko, H. Shang «A neural network-based soft sensor for particle size distribution using image analysis», Powder Technology, 212, 359–366, 2011.

[35] A. Slowik «Application of an Adaptive Differential Evolution Algorithm With Multiple Trial Vectors to Artificial Neural Network Training», IEEE Transactions on Industrial Electronics, 58, 3160-3167, 2011.

[36] M. Liu, Y. Yang, Q. Li, H. Zhang «Parallel computing of multi-scale continental deformation in the western united states: Preliminary results», Physics of the Earth and Planetary Interiors,163, 35–51, 2007.

[37] D. Marquardt «An algorithm for least squares estimation of non-linear parameters», Journal of the Society for Industrial and Applied Mathematics, 431-441,1963.

[38] M. Jalali-Heravi, M. Asadollahi-Baboli, P. Shahbazikhah «QSAR study of heparanase inhibitors activity using artificial neural networks and Levenberg-Marquardt algorithm», European Journal of Medicinal Chemistry, 43, 548-556, 2008.

[39] H. Miura, T. Takahashi, J. Ichikawa, Y. Kawase «Bed expansion in liquid–solid two-phase fluidized beds with Newtonian and non-Newtonian fluids over the wide range of Reynolds numbers». Powder Technology,117, 239–246, 2001.

[40] J.T. Ford, M.B. Oyeneyin «The Formulation of Milling Fluids for Efficient Hole Cleaning: An Experimental Investigation». SPE paper 28819, presented at the European Petroleum Conference, London, UK, 25 – 27, 1994.

نشریه فناوری نفت، گاز و پتروشیمی ۶ (۱): ۱-۱۴، تابستان ۱۳۹۸

مقاله تحقیقاتی

به کارگیری روش شبکه عصبی مصنوعی برای پیشبینی سرعت حدی سقوط ذرات غیرکروی در سیالات نیوتنی و غیرنیوتنی

آزاده میروکیلی[1*]. هدیه روحیان[2]. سیاوش چاهی‌بخش[1]

۱. ایران، بوشهر، دانشگاه خلیج فارس، دانشکده نفت، گاز و پتروشیمی

۲. ایران، شیراز، دانشگاه شیراز، دانشکده نفت و شیمی، مرکز تحقیقات میحطزیستی صنایع نفت و پتروشیمی

مشخصات مقاله

تاریخچه مقاله:

دریافت ۲۱ فروردین ۱۳۹۸

دریافت پس از اصلاح ۲۷ تیر ۱۳۹۸

پذیرش نهایی ۳ مرداد ۱۳۹۸

کلمات کلیدی:

شبکه عصبی مصنوعی

سرعت حدی سقوط

ذرات غیرکروی

سیالات غیرنیوتنی

* عهده‌دار مکاتبات؛

آزاده میروکیلی

رایانامه: mirvakili@pgu.ac.ir

gmail.com@mirvakili96

تلفن: ۰۷۷۳۱۲۲۲۶۳۲

چکیده

امروزه مطالعه بر روی سرعت حدی سقوط ذرات غیرکروی به دلیل نقش چشمگیری که در بسیاری از فرایندهای جداسازی ایفا میکند، یکی از امیدوارکنندهترین موضوعات در بحث فناوری رسوبگذاری است. در این مطالعه، پتانسیل شبکه عصبی مصنوعی (ANNs) برای پیشبینی سرعت حدی سقوط ذرات غیرکروی در مایعات نیوتنی و غیرنیوتنی با استفاده از ۳۶۱ داده آزماشگاهی بررسی شده است. شبکه عصبی مصنوعی توانسته است به دلیل قدرت پیشبینی خوب، سادگی، انعطافپذیری، ظرفیت بالا، و توانایی استفاده از تعداد زیادی الگوریتم تمرینی، عنوان محبوبترین مدل ریاضیاتی غیرخطی را به خود اختصاص دهد. مدل شبکه هوش مصنوعی توسعه یافته به منظور استفاده در این مطالعه، مقادیر پیشبینی شده قابل قبولی را برای سرعت حدی سقوط به دست آورد. مقادیر پیشبینی شده دارای خطاهای MSE، R^2، و MRE به ترتیب برابر با ۰/۹۷۲۹، ۰/۰۰۲۳، و ۲۱٪ بودند. در یک بررسی روی سرعت حدی حدی و ضریب پسار برای ذرات کروی و غیرکروی، نتایج اینگونه به دست آمد که سرعت حدی سقوط ذرات غیرکروی برابر با ۰/۱ سرعت حدی سقوط ذرات کروی است.

نحوه استناد به این مقاله:

Mirvakili A, Roohian H, Chahibakhsh S. Artificial neural network approach for the prediction of terminal falling velocity of non-spherical particles through Newtonian and non-Newtonian fluids. Journal of Oil, Gas and Petrochemical Technology, 2019; 5(2): 1-14. DOI: 10.22034/JOGPT